

## LA-UR-19-29553

Approved for public release; distribution is unlimited.

Title: Monitoring an Electro-Refining Process: Revision 1

Author(s): Fugate, Michael Lynn  
Key, Brian P.  
Tutt, James Robert

Intended for: Report

Issued: 2019-09-23

---

**Disclaimer:**

Los Alamos National Laboratory, an affirmative action/equal opportunity employer, is operated by Triad National Security, LLC for the National Nuclear Security Administration of U.S. Department of Energy under contract 89233218CNA000001. By approving this article, the publisher recognizes that the U.S. Government retains nonexclusive, royalty-free license to publish or reproduce the published form of this contribution, or to allow others to do so, for U.S. Government purposes. Los Alamos National Laboratory requests that the publisher identify this article as work performed under the auspices of the U.S. Department of Energy. Los Alamos National Laboratory strongly supports academic freedom and a researcher's right to publish; as an institution, however, the Laboratory does not endorse the viewpoint of a publication or guarantee its technical correctness.

# Monitoring an Electro-Refining Process: Revision 1

Mike Fugate, Brian Key, and James Tutt

Los Alamos National Laboratory

30 September 2019

## 1 Introduction

In this report we examine measurements from two different sensors for detecting a diversion of plutonium in an electro-refining (ER) process. One method is based on counts from a high dose neutron detector (HDND). The other is based on spectra from a micro-calorimeter sensor. The spectra come from ER-salt, fission product waste, and from a source term. The goal is to differentiate between normal and off normal operating conditions using neutron counts or changes in counts in the spectra. Unfortunately, there is no electro-refining process that we can actually monitor to obtain real data from various operating conditions so we will use simulated data to illustrate our approach.

Some related and possibly useful references are [1] and [2] and [3]. Monitoring an ER process with a micro-calorimeter sensor and different data than used here can be found in [1]

and [2]. Tutt *et al.* [3] provide a lengthy discussion high dose neutron detector simulations.

## 2 Statistical Detection of Diversion with a HDND

In this section we consider a statistical approach for detecting a diversion of Pu by counting neutrons with a HDND. We consider process monitoring for a pure uranium product and for a U/TRU product.

For a pure uranium ingot and no background, we expect the neutron count rate to be about 7.9 pulses/sec. If 1% plutonium is diverted to the ingot we expect the count rate to be about 36.8 pulses/sec.

For the U/TRU product, under normal operating conditions and no background, we expect the count rate to be about 66098.1 pulses/sec and if 1% Pu is diverted we expect the count rate to be about 64640.4 pulses/sec.

### 2.1 Detecting Diversion for U Product

For the remainder of this section consider just the case of the uranium ingot. If we monitor the process with a HDND for say, 5 minutes, the mean count rates for normal operation and 1% Pu diversion are 2370 pulses/300sec and 11040 pulses/300sec, respectively. If counts can be modeled by a Poisson distribution the standard deviation of counts is the square root of 2370 or about 49 pulses/300sec (assuming no diversion and a 5 minute count time). Clearly, if we observe counts on the order of 11040 in a 5 minute interval we have observed something

quite unusual; 11040 is about 178 standard deviations above the no diversion mean of 2370.

If neutron counts can be modeled reasonably well by a Poisson distribution the discussion in the previous paragraph suggest using the statistic

$$Z = \frac{\text{observed} - \text{expected}}{\sqrt{\text{expected}}}$$

to detect a difference in counts. Here “expected” is the no diversion mean count rate and “observed” is the measured count rate. If there is a diversion of Pu the observed count rate will be larger than what is expected under normal operation and the observed value of  $Z$  will be large. To quantify what constitutes a large observed count we need to know the distribution of  $Z$  when there is no diversion.

For the examples we consider in this report if there is no diversion and the count time is at least 5 minutes, standard statistical theory can be used to show that  $Z$  will have an approximate (standard) Gaussian distribution with mean 0 and variance 1. Quantiles of the standard Gaussian can be used to set a threshold to distinguish between typical no diversion count rates and unusual count rates. Choosing a particular threshold determines a process monitoring false alarm rate. For example, the 95th quantile of the standard Gaussian is 1.645. If we choose 1.645 as the threshold and there is no diversion, then 95% of the time  $Z$  will be less than 1.645 and 5% of the time  $Z$  will be greater than the threshold, which implies that 5% is the false alarm rate.

For the example above with a 5 minute count time and a 1% diversion of Pu, on average  $Z$  will be

$$Z = \frac{(5 \cdot 60 \cdot 36.8) - (5 \cdot 60 \cdot 7.9)}{\sqrt{5 \cdot 60 \cdot 7.9}}$$

$$= \sqrt{300} \cdot \frac{(36.8 - 7.9)}{\sqrt{7.9}} \approx 178.$$

A value of 178 is highly unusual if there is no diversion (the 99.999th quantile of a standard Gaussian is about 4.26). Either we observed something extremely rare or there was a diversion.

Note that the last equation above shows how count times influence  $Z$  and ultimately the probability of detection. For count time  $T$  we have

$$Z = \frac{\sqrt{T}(\text{observed} - \text{expected})}{\sqrt{\text{expected}}}.$$

Clearly, as count time increases the ability to detect a difference between observed and expected counts increases.

The above discussion considered only the case of a 1% diversion and no background noise. More generally, we would like to know the probability of detection for different diversion amounts and also what effect background has on the probability of detection.

Ideally, to estimate the probability of detection, we would actually perform many physical experiments where Pu was diverted in the electro-refining process, count the neutrons and see how often  $Z$  detected a significant difference. As this is not possible we will use simulations to estimate the probability of detection for various count rates and different backgrounds.

## 2.2 Estimated Probability of Detection

In this section we describe the algorithm used to estimate the probability of detection (PD) for various diversion count rates and background rates. For the uranium product, any

diversion of Pu will lead to an increase in the count rate. For the U/TRU product a diversion of Pu will lead to a decrease in the count rate.

The following lists give the parameters that need to be set for each simulation and the steps involved in estimating the PD. In the results presented below we used three different backgrounds for the U product and three for the U/TRU product.

### Parameters Set by User:

- $Q$  quantile from standard Gaussian distribution that determines the false alarm rate (e.g. choose 1.645 for a 5% false alarm rate)
- $S_0$  the mean count rate for normal operating conditions (either 7.9 or 66098.1 pulses/sec)
- $S_1$  the mean count rate when some amount of Pu has been diverted (pulses/sec)
- $B$  the mean count rate for the background (pulses/sec)
- $T$  the time to count neutrons in seconds (we used 300 and 600)

### Simulation Steps:

1.  $\mu_0 = (S_0 + B)T$ , the no diversion mean count rate in a unit of time  $T$
2.  $\mu_1 = (S_1 + B)T$ , the diversion mean count rate in a unit of time  $T$
3. Simulate  $N$  pseudo-random Poisson counts with mean  $\mu_1$ . Let  $w_i$  be the observed count from simulation  $i$ , for  $i = 1, \dots, N$  (we used  $N = 100000$ )
4. Calculate  $Z_i = (w_i - \mu_0)/\sqrt{\mu_0}$ , for  $i = 1, \dots, N$

5. Estimate the probability of detection (PD) as the fraction of times  $Z_i$  is greater than the threshold  $Q$
6. Note, if  $\mu_1 = \mu_0$  the PD should be very close to the false alarm rate with any difference due to simulation error. As  $N$  gets large this error should approach 0.

In the following sections we show probability of detection rates for the U and U/TRU products. Because the two products have very different mean count rates the simulation parameters need to be quite different.

### 3 U Product

This section shows estimated probability of detection for the U product. Recall that a 1% diversion of Pu will result in a count rate of 36.8 pulses/sec, which is quite easy to detect, even in the presence of significant background noise. To make results a little more interesting we decided to use diversion count rates from 8 to 9 pulses/sec. The following list gives the parameters of the simulation.

- Normal (no diversion) count rate: 7.9 pulses/sec
- Background: none, 100% of normal (or 7.9 pulses/sec) and 200% of normal (or 15.8 pulses/sec)
- Diversion count rates (pusles/sec): 10 equally spaced values from 7.9 to 9. Note that 7.9 corresponds to no diversion.



- Count time: 5 and 10 minutes
- False alarm rate: 5%
- Number of simulations: 100000

Figure 1 shows the probability of detection for the various scenarios plotted as a function of the no background count rates. The dashed curves correspond to 5 minute count times and the solid curves correspond to 10 minute count times. Curves of the same color have the same background count rate.

Comparing two curves of the same color shows that the PD is higher for longer count times. Comparing solid curves of different colors or dashed curves of different colors shows that the PD is higher for lower background counts. As expected, higher count times and lower backgrounds result in higher PD. Note that the dashed blue curve and the red solid curve are essentially the same. This says that counting for 5 minutes with no background (dashed blue) gives the same PD as counting for 10 minutes when background is 7.9 pulses/sec (solid red).

Each circle on a curve is a PD for a particular simulation scenario. The PD is estimated by counting how many times the statistic  $Z$  exceeds some threshold. Figure 2 shows a histogram of all the values for one scenario. This particular scenario has a 10 minute count time and a diversion count rate with no background of 8.14 pulses/sec. Every point on every curve in Figure 1 has a similar histogram.

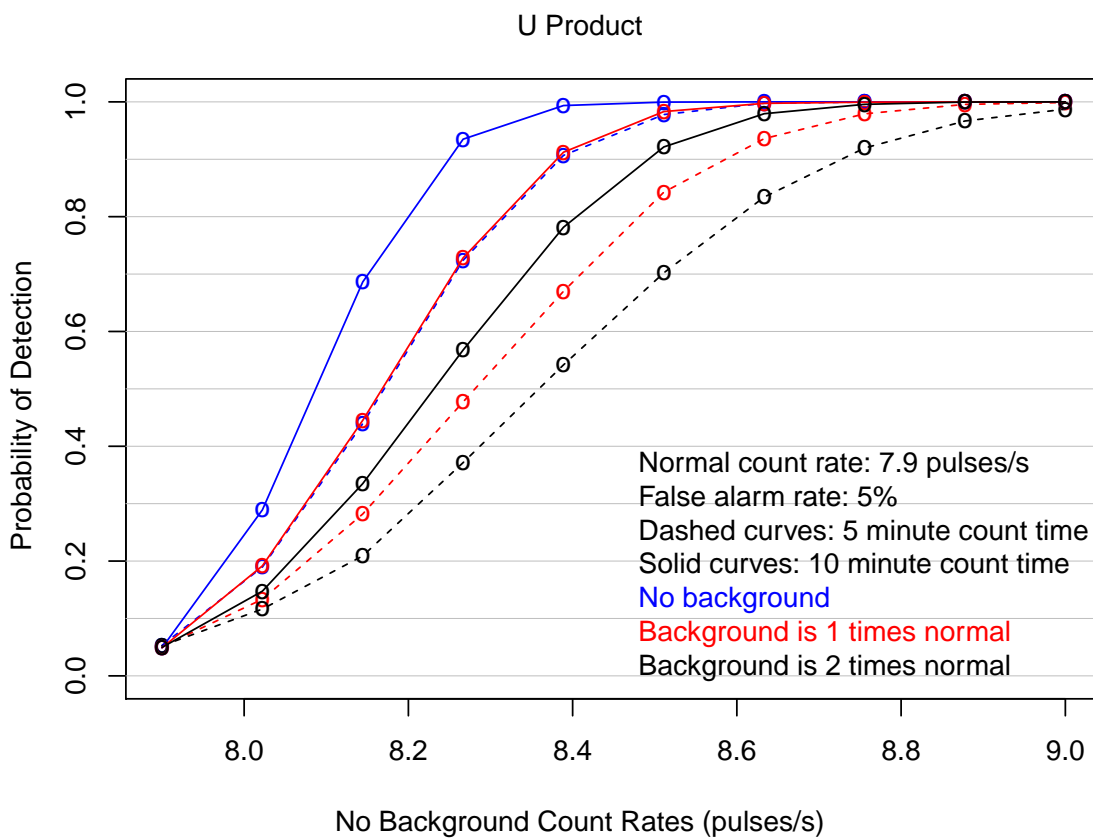


Figure 1: Probability of detection for various count rates, times, and backgrounds. Curves of the same color have the same background count rate. Note that the dashed blue curve plots under the solid red curve.

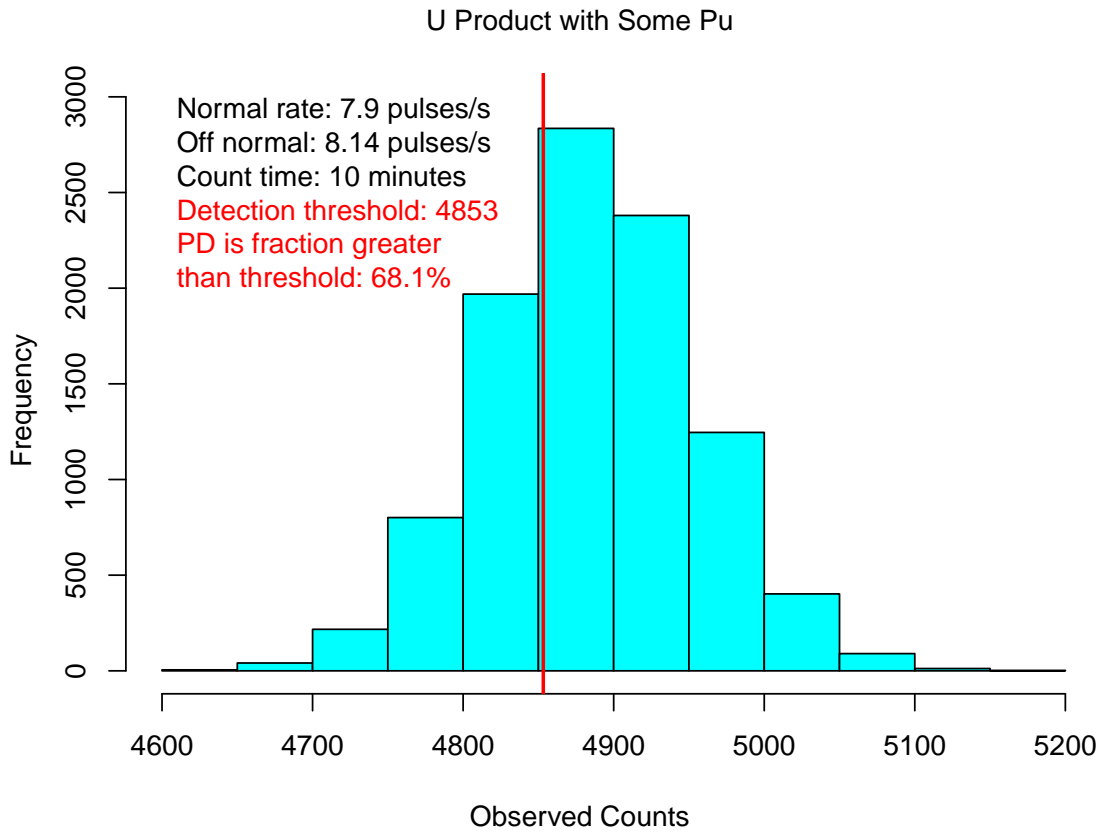


Figure 2: Observed counts for one off normal rate and no background. Compare to the third circle on the solid blue curve in the previous figure.

### 3.1 Probability of Detection for Small Diversions

This section shows detection probabilities when the amount of plutonium diverted is 0.02% or less. To estimate a detection probability for a given amount diverted we need the count rate associated with the percent diverted. Table 1 shows count rates for various percents diverted. These rates were calculated by evaluating the neutron source term for each diversion case and performing MCNP simulations of the HDND response to determine count rate, see Tutt et al. 2018. Count rates for other percents were determined by linear interpolation between 0% and 0.25%.

Table 1: Percent plutonium diverted for the uranium ingot and corresponding count rates.

Percent Diverted	Pulses/sec
0	7.9
0.005	8.096
0.010	8.153
0.250	13.34
0.750	23.72
1.0	36.8

Figure 3 shows the probability of detection when the percent of plutonium diverted is from 0.002% to 0.02%. We show results for 5 counting times and 4 backgrounds (no background interference and 3 background count rates). As expected, when the amount diverted decreases the probability of detection also decreases. However, if the counting time is sufficiently long, the probability of detection is reasonable.

Figure 4 shows the same curves but arranged by count time. This shows how, for a given counting time, the probability of detection decreases as the background count rate increases. Again, this is not surprising.

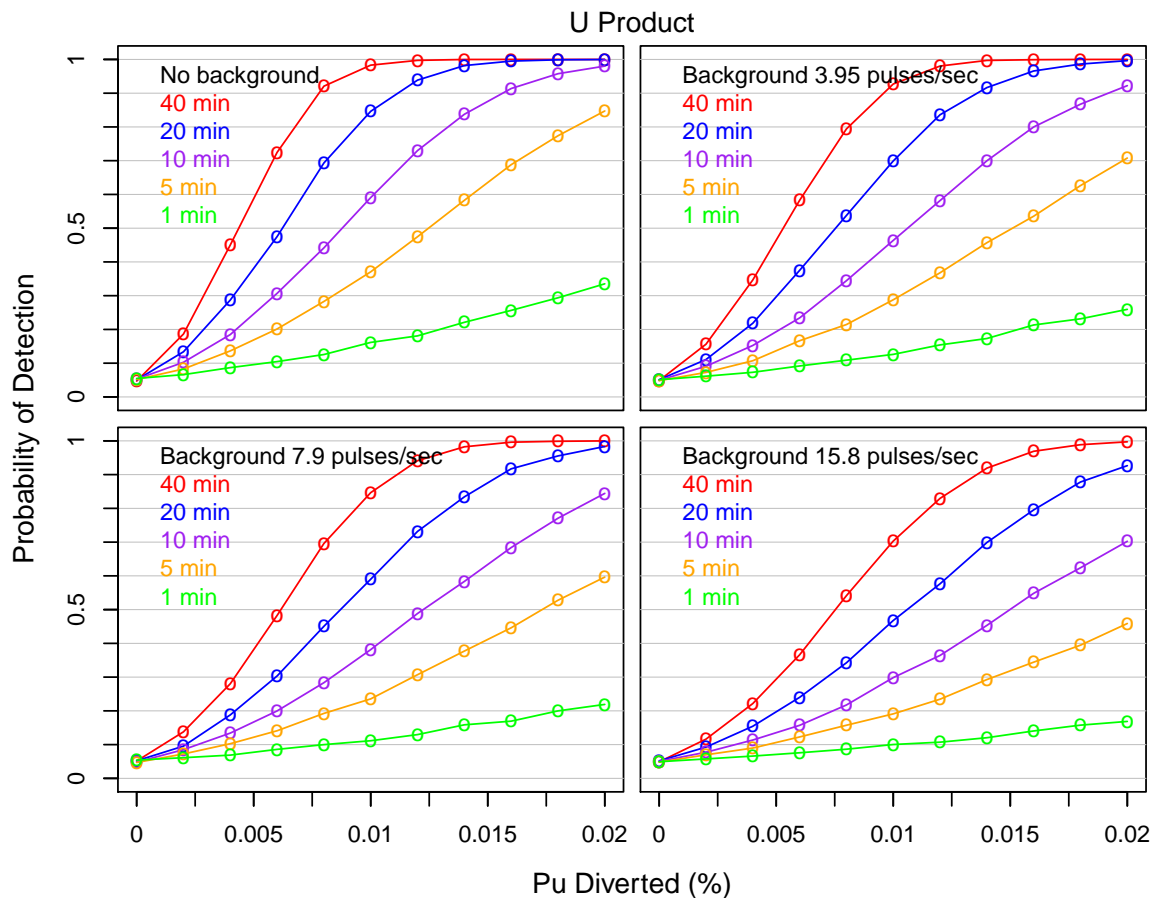


Figure 3: Probabilities of detection with 4 backgrounds and 5 counting times.

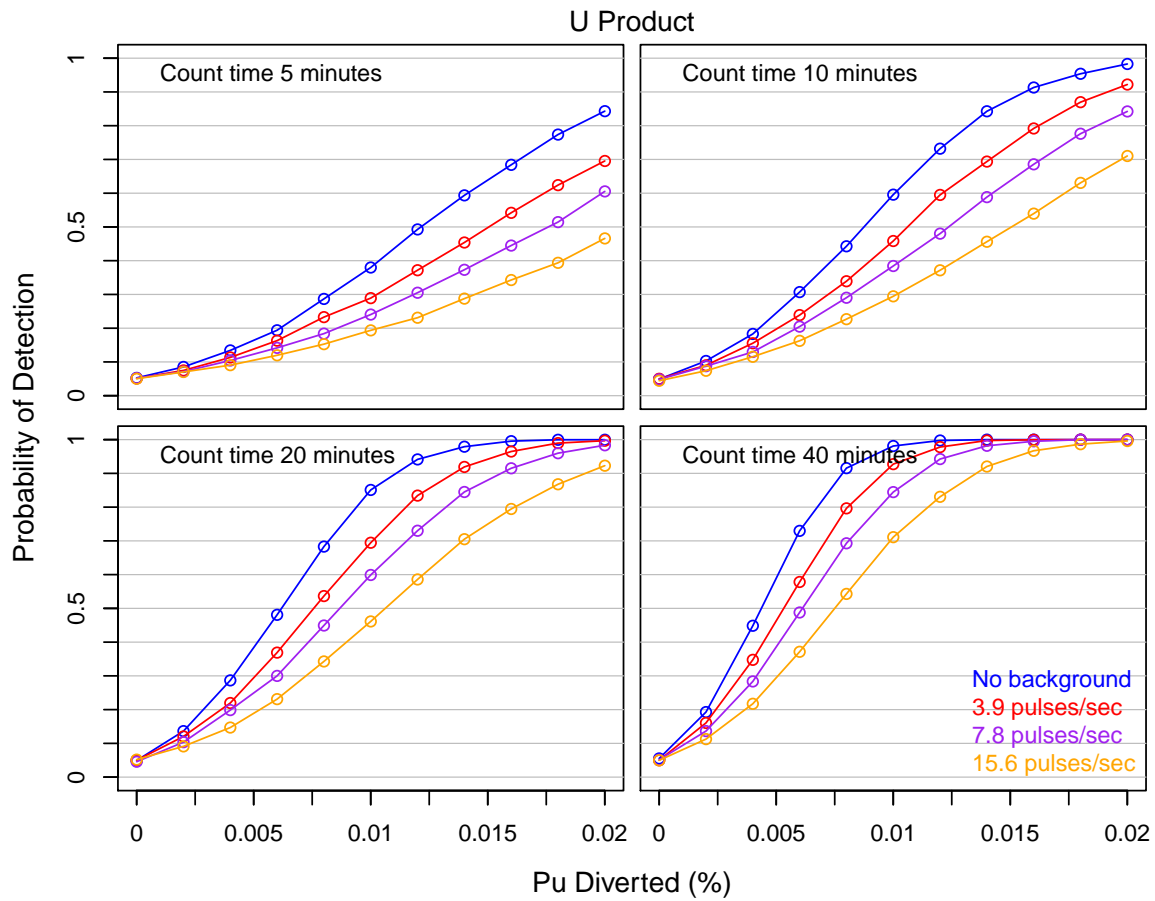


Figure 4: Probabilities of detection for a given count time and 4 backgrounds.

## 4 U/TRU Product

This section shows estimated probability of detection for the U/TRU product. Recall that a 1% diversion of Pu will result in a count rate of 64640.4 pulses/sec, which is quite easy to detect, even in the presence of significant background noise. Because count rates are so high, relatively small difference in rates can be detected quite easily. Because of this we decided to examine what effect very high background rates have on the PD. The following list shows the parameters of the simulation.

- Normal (no diversion) count rate: 66098.1 pulses/sec
- Background: none, 20 *times* normal and 50 *times* normal
- Diversion count rates (pusles/sec): 10 equally spaced values from 64640.4 to 66098.1.  
Note that 66098.1 corresponds to no diversion.
- Count time: 5 and 10 minutes
- False alarm rate: 5%
- Number of simulations: 100000

Figure 5 shows the probability of detection for the various scenarios plotted as a function of the no background count rates. The dashed curves correspond to 5 minute count times and the solid curves correspond to 10 minute count times. Curves of the same color have the same background count rate.

The reason background rates have to be so high to see some difference in PD is because, with Poisson data, the standard deviation is the square root of the mean and, compared to the mean, the square root of the mean is relatively small when counts are large. Also, if we look at the form of the  $Z$  statistic we can see just how unusual a count of 64640.4 is relative to the no diversion mean count rate of 66098.1

$$Z = \frac{(66098.1 - 64640.4)}{\sqrt{66098.1}} \approx 5.7.$$

In other words, a count rate of 64640.4 is about 5.7 standard deviations from the mean rate of 66098.1. So, if we count for even a small amount of time the difference becomes highly significant. For example, if we count for 5 minutes the  $Z$  value is  $\sqrt{300}(5.7)$ , or about 98 standard deviations from the no diversion mean.

Continuing further, if the background rate is  $X$  times the no diversion rate and the count time in seconds is  $T$ , then on average we will have

$$\begin{aligned} Z &= \frac{\sqrt{T}((X+1)\text{expected} - (\text{observed} + X(\text{expected})))}{\sqrt{(X+1)\text{expected}}} \\ &= \frac{\sqrt{T}(\text{expected} - \text{observed})}{\sqrt{X+1}\sqrt{\text{expected}}}. \end{aligned}$$

If there is no background then  $X$  is 0 and this is the  $Z$  statistic above (with observed and expected switched in the numerator). The last line shows the benefit of long count times.



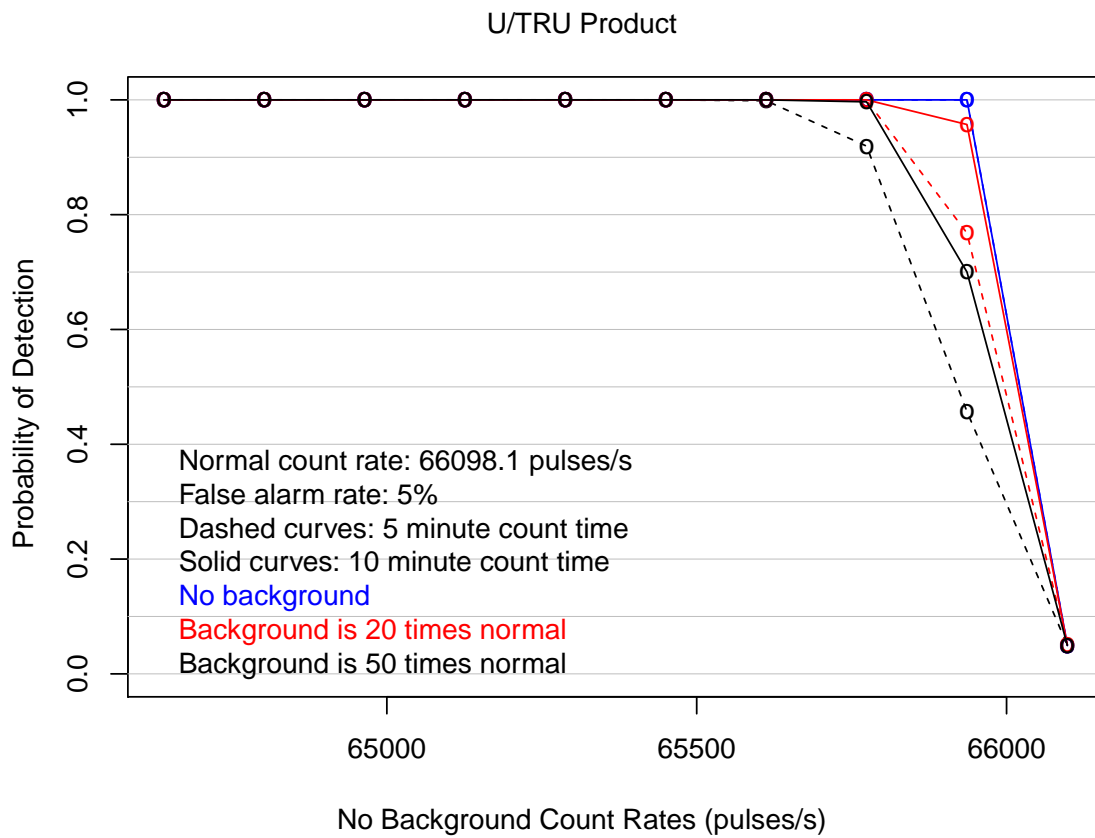


Figure 5: Probability of detection for various count rates, times, and backgrounds. Curves of the same color have the same background count rate. Note that the dashed blue curve plots under the solid red curve.

## 5 Detecting Diversion with a Micro-Calorimeter Sensor

In this section we look at using spectra from a micro-calorimeter sensor to detect a diversion. Spectra are obtained (simulated) for ER-salt, fission product waste, and source terms.

### 5.1 Micro-Calorimeter Spectra for ER-Salt

This section looks at detecting a diversion in the ER-salt. Figure 6 shows four high intensity gamma lines that correspond to isotopes we used in a previous study. Figure 7 shows detection probabilities for a 5% false positive rate when 1% and 1.5% Pu is diverted. Because counts are so high for these four peaks we only used the relatively low count Eu-155 peak at 105.31 keV to estimate detection probabilities. Clearly, using any of the higher count peaks would have resulted in higher detection probabilities for the same diversion percent.

Reference previous report for methodology used to generate PDs.

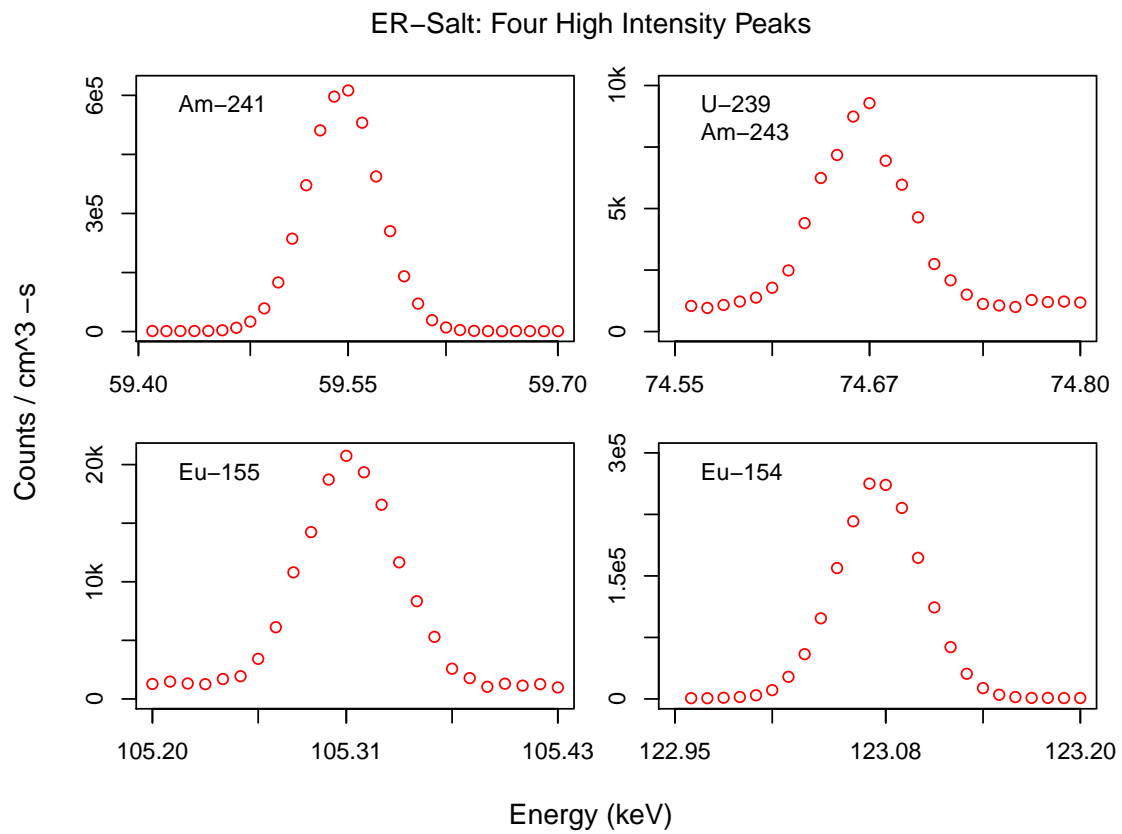


Figure 6: ER-salt isotopes of interest.

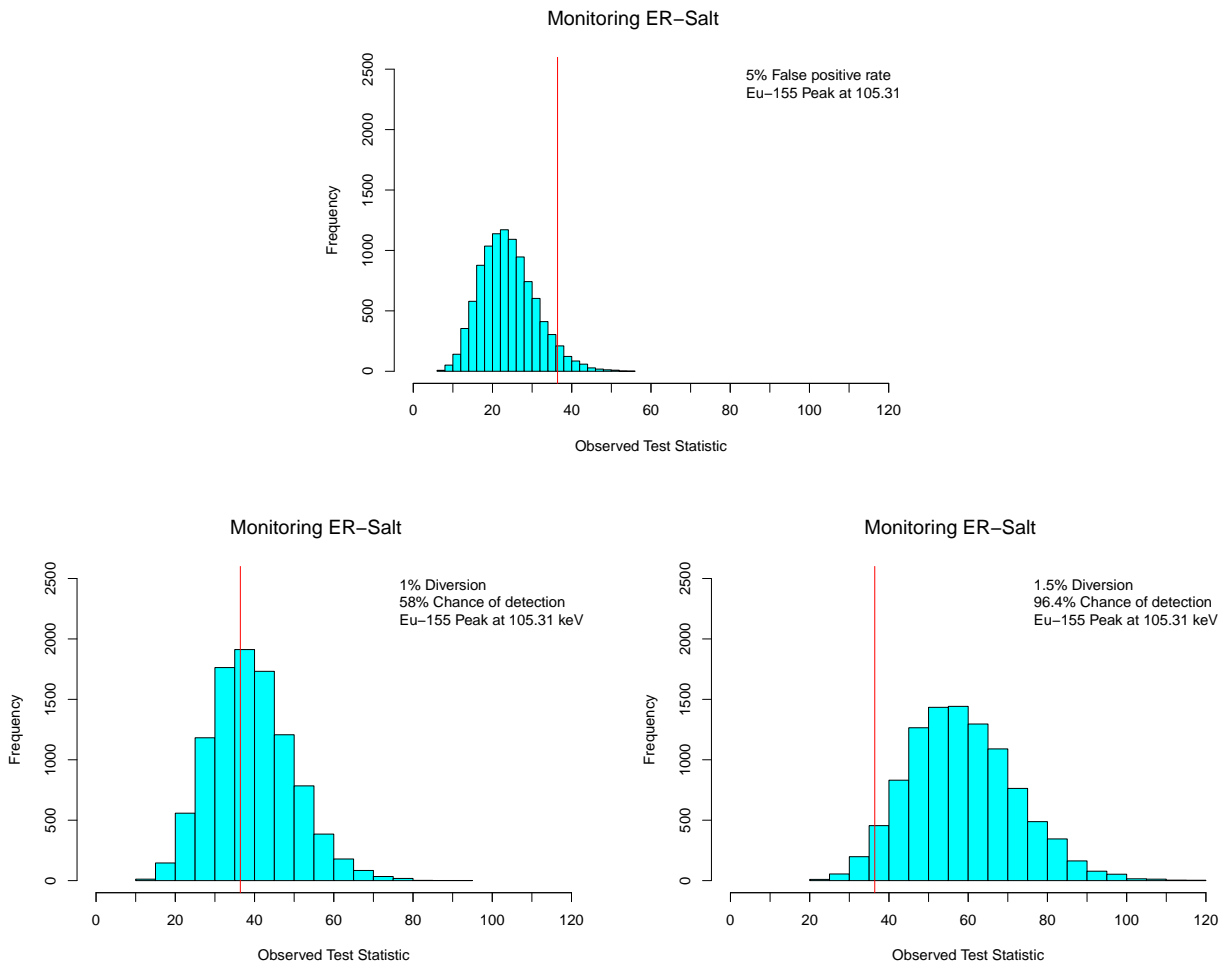


Figure 7: Monitoring ER-salt with Eu-155 counts at 105.31 keV.

## 5.2 Micro-Calorimeter Spectra for Source Term

This section looks at detecting a diversion in the source term. Figure 8 shows ten high intensity gamma peaks from the source term. For almost all of the isotopes, it's hard to tell what energy bin contains the “peak”. If a peak isn't well defined it will be hard to use that peak for detecting a diversion.

For illustration consider the the data in the top panel of Figure 9. The Np-239 peak is supposed to be at 106.12 keV and there are two high counts near this energy. But how many data points on each side of 106.12 actually belong to the peak is hard to say. And including data that is essentially just noise is going to lower the detection probability.

The bottom plots in Figure 9 shows detection probabilities for two scenarios. For both scenarios the signal is between 106.06 and 106.18, which corresponds to the data between the blue lines in the top panel. The bottom left plot shows a histogram of values of the test statistic when we include noise data from 105.8 to 106.44 (solid black lines). The probability of detecting a diversion is about 32%. The bottom right plot is similar but we only include noise data from 106.02 to 106.22 (dashed black lines). The probability of detecting a diversion is now about 59%. This illustrates the importance of being able to define the regions of interest.

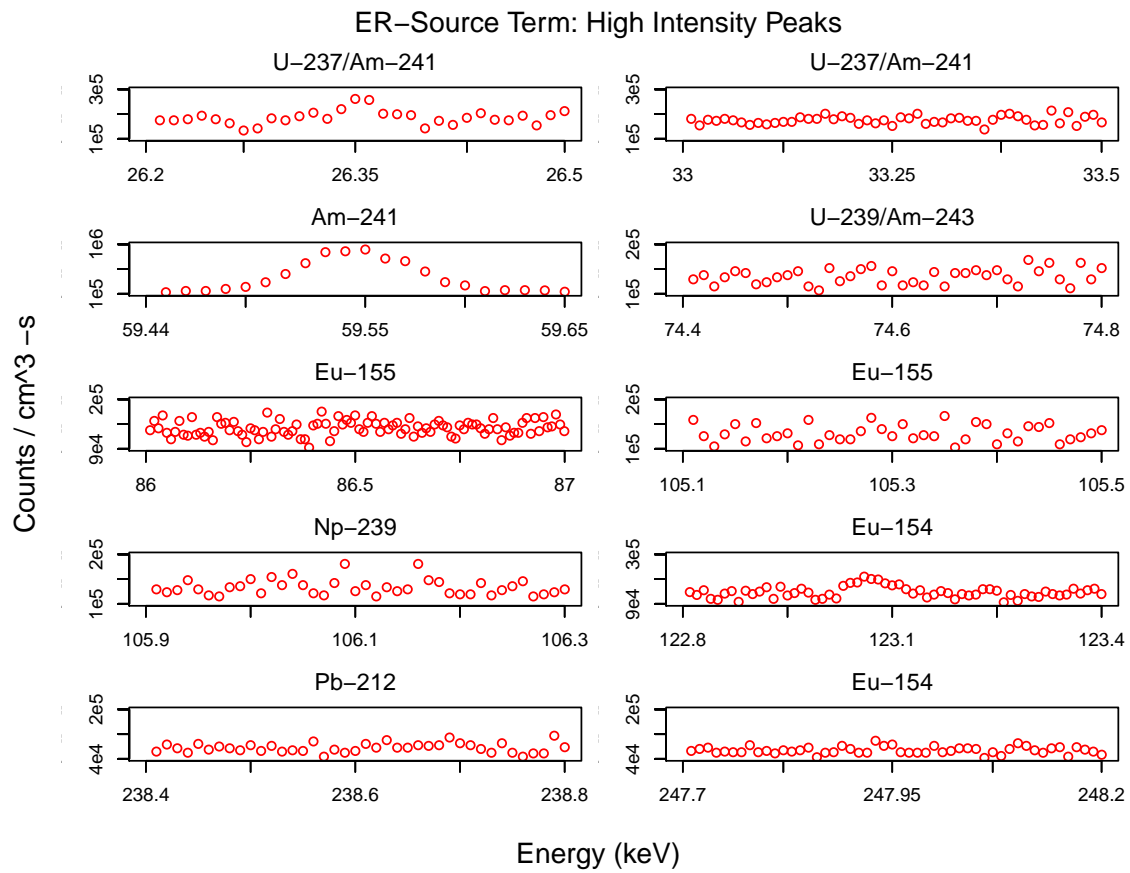


Figure 8: ER source term isotopes of interest.

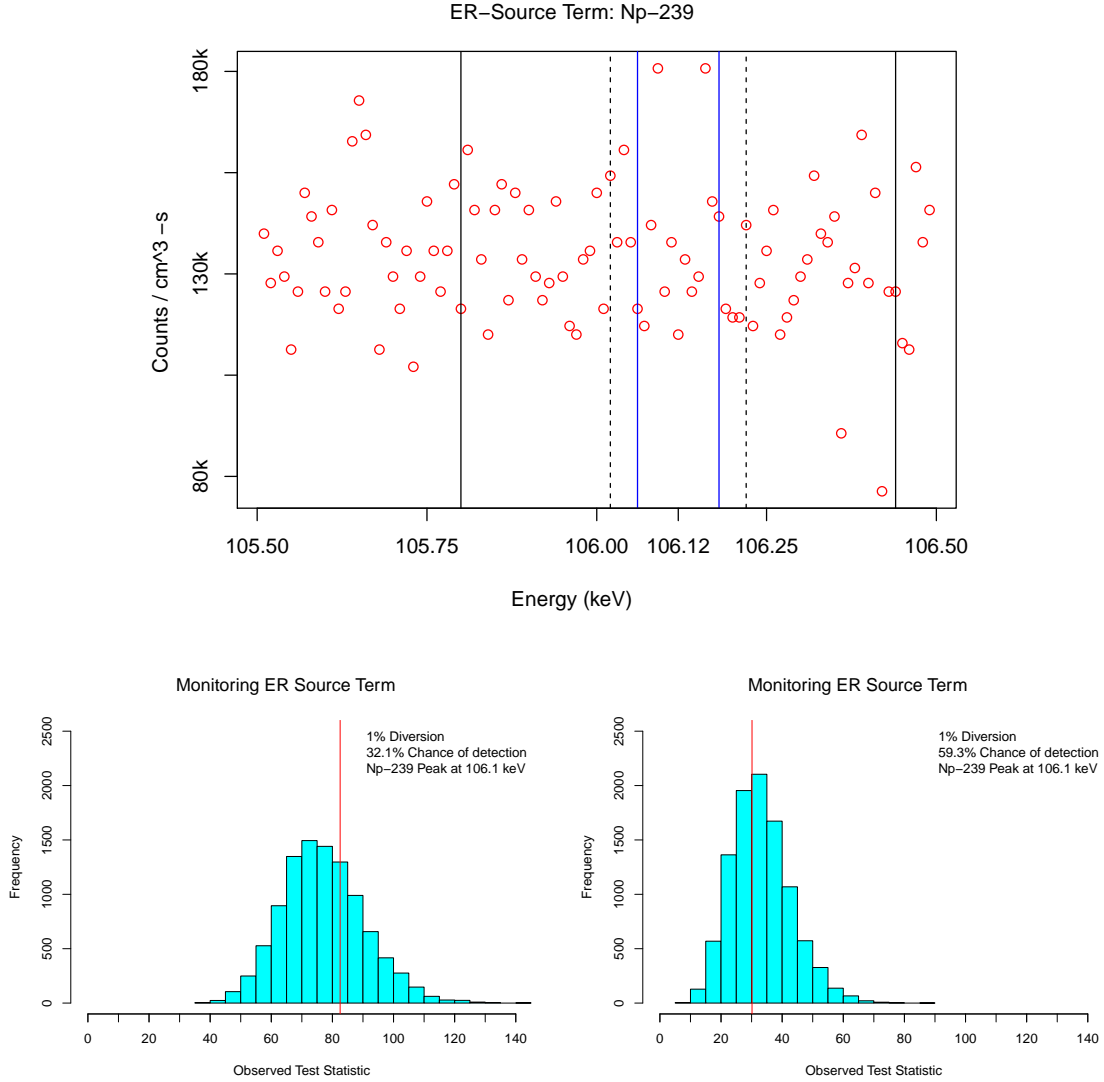


Figure 9: Top panel shows data around the Np-239 peak at 106.12. To estimate a probability of detection (PD) we defined the signal to be between 106.06 and 106.18 (solid blue lines). The bottom left panel shows the PD when we include noisy counts between the solid black lines and the blue lines. The bottom right panel shows the PD when the noisy counts are between the dashed black lines and the blue lines.

## References

- [1] Brian P. Key, Michael L. Fugate, Eric B. Rauch, P. Croce, Mark, Laura A. Limback, and et al. Advanced integration methods for monitoring an electro-refining process. *Los Alamos National Laboratory Report*, LA-CP-18-20204, 2018.
- [2] Brian P. Key, James R. Tutt, and Michael L. Fugate. Advanced integration. *Los Alamos National Laboratory Report*, LA-UR-18-28521, 2018.
- [3] James R. Tutt, Michael L. Fugate, and Brian P. Key. Advanced integration of high dose neutron, microcalorimeter and voltammetry sensor technologies in an electro-refining process. *Los Alamos National Laboratory Report*, LA-UR-18-29076, 2018.